Mechanism-independent method for predicting response to multidrug combinations in bacteria

Kevin Wood[a], Satoshi Nishida[a], Eduardo D. Sontag[b], and Philippe Cluzel[a,1]

[a]FAS Center for Systems Biology, Department of Molecular and Cellular Biology, School of Engineering and Applied Sciences, Harvard University, Cambridge, MA 02138; and [b]Department of Mathematics, Rutgers University, Piscataway, NJ 08854

Edited by Jonathan S. Weissman, University of California, San Francisco, CA, and approved June 1, 2012 (received for review January 23, 2012)

Drugs are commonly used in combinations larger than two for treating bacterial infection. However, it is generally impossible to infer directly from the effects of individual drugs the net effect of a multidrug combination. Here we develop a mechanism-independent method for predicting the microbial growth response to combinations of more than two drugs. Performing experiments in both Gram-negative (*Escherichia coli*) and Gram-positive (*Staphylococcus aureus*) bacteria, we demonstrate that for a wide range of drugs, the bacterial responses to drug pairs are sufficient to infer the effects of larger drug combinations. To experimentally establish the broad applicability of the method, we use drug combinations comprising protein synthesis inhibitors (macrolides, aminoglycosides, tetracyclines, lincosamides, and chloramphenicol), DNA synthesis inhibitors (fluoroquinolones and quinolones), folic acid synthesis inhibitors (sulfonamides and diaminopyrimidines), cell wall synthesis inhibitors, polypeptide antibiotics, preservatives, and analgesics. Moreover, we show that the microbial responses to these drug combinations can be predicted using a simple formula that should be widely applicable in pharmacology. These findings offer a powerful, readily accessible method for the rational design of candidate therapies using combinations of more than two drugs. In addition, the accurate predictions of this framework raise the question of whether the multidrug response in bacteria obeys statistical, rather than chemical, laws for combinations larger than two.

pairwise | entropy | prokaryotes | dose-response relationship

Combinations of three or more drugs have been studied in both clinical and laboratory settings as potential treatments for severe microbial infections (1–4). Drug interactions, including those that are clinically beneficial, have typically been studied using descriptive, rather than predictive, approaches that quantify the effects of a given drug pair on growth (5–7). For example, two drugs whose effects on microbial growth counteract one another, when used in combination, are known as antagonistic, whereas drugs whose potencies are significantly increased in combination are referred to as synergistic. As a result of these interactions, the effects of drug combinations cannot, in general, be predicted based on the effects of the drugs alone (7). Although combinations of two drugs have been studied extensively, little is known about the way in which more than two drugs combine to yield higher-order effects on bacterial growth, which is the relevant clinical outcome in treatments of bacterial infections. Here, we ask if it is possible to understand and to predict the effects of these larger drug combinations without relying on specific mechanistic details but rather on principles shared by a large number of biological systems.

For example, consider a classic three-drug combination of chloramphenicol (a protein synthesis inhibitor), ofloxacin (a fluoroquinolone DNA synthesis inhibitor), and trimethoprim (a folic acid synthesis inhibitor) at the following concentrations: [chloramphenicol]=1.5 μg/mL, [ofloxacin]=40 ng/mL, and [trimethoprim]=0.3 μg/mL. The growth rate of *E. coli* treated with each drug alone is about 0.58, 0.47, and 0.39 (normalized by the growth of untreated cells), respectively. Combining chloramphenicol and ofloxacin leads to a growth rate of 0.53, which is significantly higher than expected from a naive multiplication of the single drug rates (0.27) and consistent with previously observed antagonism between DNA synthesis inhibitors and protein synthesis inhibitors (8). On the other hand, combining ofloxacin with trimethoprim completely eradicates growth (growth < 0.01, compared with 0.18 expected from single drug growth rates), consistent with previously reported synergy between trimethoprim and fluoroquinolones (9). Finally, the combination of chloramphenicol and trimethoprim leads to a growth rate of 0.16, slightly smaller than the 0.23 predicted from single drug growth rates. The effects of all three *pairs* of drugs differ significantly from that predicted by multiplication of single drug effects. Therefore, there is seemingly little hope that such an assumption of independence will be useful when all three drugs are combined and the chemical complexity of the problem is increased. Surprisingly, the growth rate in the presence of all three drugs (0.11) is equal to the product of single drug growth rates, suggesting that the drugs act independently. Why have the previously strong interactions between drug pairs been eliminated when the three drugs are combined, leading to a mixture of effectively independent drugs? One hypothesis would be that the net effect of the drug combination arises from compensatory interactions that can only be measured when all three drugs are present. Alternatively, the net effect could follow directly from the accumulation of interactions between pairs of drugs. We wish to answer this question using a quantitative framework to provide insight into how the cell integrates signals from larger drug combinations.

To tackle this question for a wide range of drug combinations, we develop a mechanism-independent model to quantify the relative contributions of combined chemical exposure—that is, one-drug effects, two-drug effects, and, in general, *N*-drug effects—to the multidrug growth response. We construct the model using a common statistical method, entropy maximization, which ensures that the model does not incorporate unwarranted statistical structure. We then test predictions of this framework using two species that represent Gram–negative (*Escherichia coli*) and Gram–positive (*Staphylococcus aureus*) bacteria. This predictive framework is a potentially powerful tool for studying multidrug effects, even without knowledge of the underlying network structure, molecular dynamics, or any other intracellular details.

Results

Response of *E. coli* to Single Drugs and Drug Pairs. First, we measured the growth of *E. coli* in the presence of a single drug and then pairs of drugs by growing liquid cultures in Luria-Bertani media. We used a large variety of drugs, including several classes of protein synthesis inhibitors (with 30S and 50S ribosomal targets), DNA synthesis inhibitors (fluoroquinolones), folic acid synthesis inhibitors, and analgesics (Table S1). Using time series of optical density measured directly from a 96-well plate reader, we estimated growth with nonlinear least-squares fitting (*Methods*,

Author contributions: K.W., E.D.S., and P.C. designed research; K.W. and S.N. performed research; K.W. and P.C. analyzed data; and K.W., S.N., E.D.S., and P.C. wrote the paper.

The authors declare no conflict of interest.

This article is a PNAS Direct Submission.

[1]To whom correspondence should be addressed. E-mail: cluzel@mcb.harvard.edu.

This article contains supporting information online at www.pnas.org/lookup/suppl/doi:10.1073/pnas.1201281109/-/DCSupplemental.

Fig. S1). We define $g_{1...N}$ to be the measured growth rate of cells in our experiments exposed to a treatment with N drugs, D_1, D_2, ..., D_N. All growth rates are normalized by growth rate in the absence of drugs. To understand the relationship between pairwise drug interactions and the net drug interaction between more than two drugs, we first asked whether one can estimate the growth response to three or four drugs using only our experimental measurements of single drug, g_i, and two-drug, g_{ij}, growth rates (Fig. 1).

We model the effect of each drug, D_i, using an associated stochastic variable, X_i. Specifically, we assume that the measured (normalized) growth rate is equal to the mean (i.e., expectation) value of that random variable, $g_i = <X_i>$. Similarly, in the presence of two drugs, i and j, the normalized growth is taken to be $g_{ij} = <X_i X_j>$ and, in general, the normalized growth in presence of a combination of N drugs, $g_{1...N}$, equals the mean value $<X_1 \ldots X_N>$ of the product of the X_is. The relevant experimental observable, growth, is associated with the moments (or joint moments) of the variables X_i, not to the stochastic variables themselves. By construction, then, drug interactions are represented as correlations between these abstract variables. In this framework, an absence of correlation between variables X_i and X_j indicates that the drugs do not interact, and therefore g_{ij} is equal to the product of the independent growth rate g_i and g_j. In the absence of interactions between the drugs, this statistical model is equivalent to the well-known Bliss independence model (5, 7) in pharmacology.

Drug Interactions Defined as a Mechanism-Independent Statistical Problem. To characterize the apparent interactions between drugs (i.e., synergies and antagonisms), we introduce a probability density $P(x) = P(x_1, x_2, \ldots, x_N)$ that describes the joint distribution of these random variables. Unfortunately, this probability distribution P(x) is not directly accessible, although as we will show, it can be estimated using experimental data. Specifically, we wish to estimate the probability density P(x) using only the growth rate data in response to single drugs and drug pairs. We call this estimate $P_{pair}(x)$, because it depends only on the interactions between drug pairs and the effects of the drugs alone. $P_{pair}(x)$ provides a picture of how the two-drug interactions would accumulate if there were no additional drug interactions, such as those requiring the presence of all three or four drugs. Of course, $P_{pair}(x)$ will provide a good approximation to the true P(x) and, ultimately, to experiments only if the effects of higher-order interactions (three-drug, four-drug) are negligible.

To estimate $P_{pair}(x)$ from experiments, we use entropy maximization (10, 11) (Fig. 1), a well-established statistical technique that guarantees that $P_{pair}(x)$ contains only the information from our one-drug and two-drug data sets (*SI Appendix*). In this case, the form of the maximum entropy distribution is given by

$$P_{pair}(x) = \frac{1}{Z} \exp\left(\sum_i h_i x_i + \sum_{i<j} J_{ij} x_i x_j \right)$$

where subscripts label the components of x, and h and J represent the collection of free parameters determined by the data (*SI Appendix*, Figs. S2–S6), and Z is the normalization constant (i.e., partition function). It is straightforward to determine the parameters h_i and J_{ij} from our measurements of single and pairwise drug effects at each dosage (*SI Appendix*).

Three- and Four-Drug Interactions Arise from Accumulation of Pairwise Interactions. Using the estimated distribution $P_{pair}(x)$, one can easily calculate the expected growth response to a larger combination of drugs, $g_{1...N} = <X_1 X_2 \ldots X_N>$, where brackets represent an average using the distribution $P_{pair}(x)$. This prediction would match experimental results only if the net effects of the drug combination were to arise entirely from the accumulation of pairwise interactions but not from higher drug interactions. To test this framework, we calculated expected growth response to various combinations of N drugs. We focus on the $n = 3$ and $n = 4$ cases, which are near the upper limit of current multidrug treatments in clinical settings. We then directly measured bacterial growth in the presence of these drug combinations

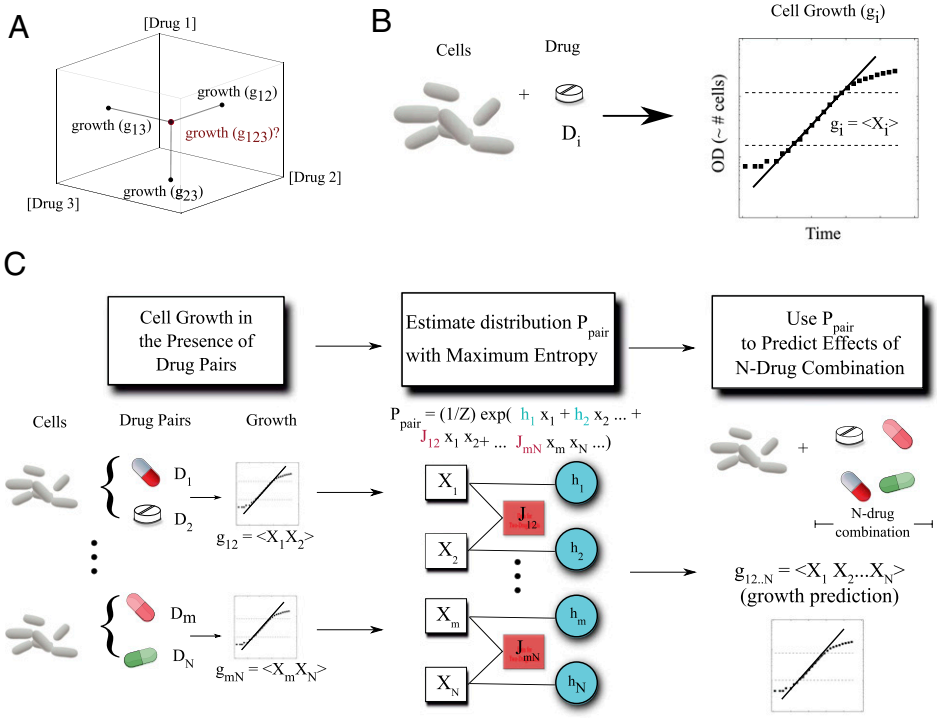

Fig. 1. Growth in response to multiple drugs can be predicted from the growth in response to those drugs singly and in pairs using maximum entropy. (*A*) Schematic axes showing that the normalized growth responses of bacteria to pairs of drugs (g_{12}, g_{23}, g_{13}) are used to predict the normalized growth response to all three drugs (g_{123}). We use the three-drug case as an example; but growth in response to any number (N) of drugs can be predicted as long as we know all pairwise responses. (*B*) We estimate growth in the presence of drugs using nonlinear least-squares fitting to optical density time series. For each drug i, we define a random variable X_i whose expectation value is equal to the growth g_i. (*C*) We made predictions by first estimating the maximum entropy distribution, P, using growth rate data from cells exposed to single drugs and drug pairs. The distribution takes an exponential form parameterized by resilience coefficients (h_i, blue circles) and drug–drug coupling coefficients (J_{ij}, pink boxes) that characterize the single drug response and the response to pairs of drugs, respectively. The resilience and coupling coefficients are chosen to ensure that the moments, $<X_i>$ and $<X_i X_j>$, of P_{pair} match the two-drug growth rate data at each drug dosage. After determining the maximum entropy distribution, the *N*-drug growth response can be predicted by calculating the expectation values of the product $X_1 X_2 \ldots x_N$. We find that these expectation values are related to the moments $<X_i>$ and $<X_i X_j>$ by simple algebraic expressions (*SI Appendix*).

and compared them to our expected results using the estimated distribution $P_{pair}(x)$. Notably, the relationship between the N-drug response and the responses to single drugs and drug pairs—a relationship governed by the distribution $P_{pair}(x)$ calculated from entropy maximization—is well described by simple algebraic expressions (12) (*SI Appendix*, Fig. S7). For example, the response to three drugs (g_{ijk}) is given by

$$g_{ijk} = g_i g_{jk} + g_j g_{ik} + g_k g_{ij} - 2 g_i g_j g_k,$$

and the response to four drugs (g_{ijkl}) is given by

$$g_{ijkl} = g_{ij} g_{kl} + g_{ik} g_{jl} + g_{il} g_{jk} - 2 g_i g_j g_k g_l$$

These well-known formulas are fully consistent with our numerical maximum entropy predictions and can be derived from the famous Isserlis theorem (12) in the specific case when $P_{pair}(x)$ is a Gaussian distribution. The simple expressions provide a way to predict the effect of a drug combination on growth without using the sophisticated maximum entropy framework. However, the fact that these simple formulas yield predictions identical (Fig. S7) to those from maximum entropy calculations guarantees that they contain no hidden correlations, only correlations from measured pairwise and single drug effects.

Fig. 2*A* shows representative data collected from bacteria exposed to various concentrations of the combination of three antibiotics, erythromycin, doxycycline, and lincomycin. All three drugs inhibit protein synthesis, erythromycin by inhibiting translocation of peptidyl tRNA, doxycycline by disrupting aminoacyl-t-RNA binding to the ribosome, and lincomycin by inhibiting enzymatic activity of peptidyl transferase. We previously found that lincomycin is antagonistic with both doxycycline and erythromycin, whereas the latter two drugs are synergistic (Fig. S2). However, because the mode of action is similar for the three drugs, it is possible that these mechanisms might interact in a unique way when all three drugs are present (see also *SI Appendix*, Fig. S8 for drugs with identical modes of action). Therefore, it is not clear whether the overall effect could be predicted solely from the accumulation of the measured pairwise interactions. Interestingly, Fig. 2*A* demonstrates that the pairwise interactions are indeed sufficient to accurately predict the growth response to the combination of these three protein synthesis inhibitors.

Next, we tested this approach using chloramphenicol, erythromycin, and salicylate. The former two drugs are protein synthesis inhibitors. The binding of chloramphenicol to its ribosomal target has been shown to enhance the ribosomal binding of erythromycin (13), and it is therefore not surprising that we found chloramphenicol and erythromycin to be synergistic when used together. Salicylate, the active component of the analgesic aspirin, is known to be a potent inducer of a multidrug efflux pump that contributes to *E. coli*'s resistance to chloramphenicol (14). Consequently, it is also not surprising that chloramphenicol and salicylate are strongly antagonistic. Although interactions between salicylate and erythromycin have not been studied, we found them to be weakly antagonistic. What happens when the three drugs are combined together? A priori, one might expect a novel effect when all three drugs are present. The presence of salicylate decreases the intracellular concentration chloramphenicol, which might then decrease the binding affinity of erythromycin in a manner that depends on the dosages of salicylate and chloramphenicol. However, we find that pairwise interactions again yield accurate predictions of multidrug effects (Fig. 2*B*).

We found similar results for three additional three-drug combinations and also for two four-drug combinations. In all experiments, the predictions from the pairwise experiments provide accurate descriptions of the data (Fig. 2*C*, Figs. S9–S15, and Table S2). Interestingly, although most *pairs* of drugs interact either synergistically or antagonistically, we found that some three-drug combinations, such as doxycycline-erythromycin-lincomycin, act almost independently in larger combinations, whereas others, such as chloramphenicol-salicylate-ofloxacin, display extremely strong interactions and deviate significantly from Bliss independence (Fig. S9). Using standard model selection techniques (*SI Appendix*, Fig. S10), we verified that the Bliss independence model may be applicable for select drug combinations, but as a whole, the pairwise model ($R^2 = 0.90$) performs significantly better than the independent model ($R^2 = 0.33$) for describing the effects of three or four drugs in combination (Figs. S11–S15). In addition to the previous results, which include drug combinations over a large range of drug dosages, we also surveyed various multidrug interactions by performing five combinatorial experiments yielding 93 unique three-drug combinations and a total of 120 unique dosage combinations (*SI Appendix*, Figs. S16 and S17 and Table S3). We included a large range of drug types, including pain relievers, food preservatives, and inhibitors of DNA synthesis, folic acid synthesis, cell wall synthesis, and protein synthesis. Again, the pairwise model ($R^2 = 0.95$) significantly outperforms the independent model ($R^2 = 0.29$) and provides an excellent description of the data. Overall, these results suggest that for a wide range of antimicrobial drugs, the net effect of a drug combination is dominated by the accumulation of pairwise drug interactions, independent of the modes of action of the specific drugs involved.

Effects of Three-Drug Combinations in *Staphylococcus aureus*. Because this approach does not rely on assumptions about molecular mechanisms, it should then be applicable to other bacterial species. As a model system, we used the bacterium *Staphylococcus aureus*, a common source of clinical infections. *S. aureus* are Gram-positive bacteria whose response to antibiotics differ substantially from that of *E. coli* (15). As for *E. coli*, we first measured the growth of *S. aureus* in response to three drugs: tetracycline, kanamycin, and erythromycin. All three drugs inhibit protein synthesis via different mechanisms. We performed the measurements for all drugs alone, and then repeated the measurement for all pairs of drugs.

Using the single drug and pairwise measurements, we then estimated the distribution $P_{pair}(x)$, which allowed us to calculate the expectation of the growth response to the three-drug combination. We tested these predictions by comparing them with direct measurements of *S. aureus* growth in the presence of all three drugs. Remarkably, Fig. 2*D* demonstrates that the mechanism-independent framework correctly predicts the experimentally measured growth response to multidrug exposure in *S. aureus* based solely on the responses to single and drug pairs.

Quantifying the Contribution of Pairwise Interactions to the Multidrug Response. Overall, these results suggest that the integrated growth response of bacteria to three-drug and four-drug combinations can be directly inferred from the measured interactions between drug pairs. The data and the predictions are in excellent agreement, and the pairwise model performs significantly better than the Bliss independence model according to model selection techniques. However, the maximum entropy framework (16, 17) provides an additional metric that allows us to further quantify exactly how well the pairwise model captures deviations from independence. To do so, we used the maximum entropy distributions P_i ($i = 1,2,3$), which are consistent with the measured effects of all combinations composed of up to i drugs, to calculate the fraction of total correlations, f_c, captured by the pairwise hypothesis (Table S4). Strikingly, this analysis demonstrates that there is very little additional information (~3%) encapsulated by pure three-drug interactions. The answer to our original question is therefore surprising: the combined effects of these three-drug combinations follow almost entirely from the effects of the drugs alone and in pairs.

How Exactly Do Pairwise Interactions Accumulate? Our results demonstrate that for a large variety of antimicrobial drug combinations, no new apparent chemical interactions arise when three or four drugs are combined together. Instead, the net effect of the drug combination arises from the cumulative effect of the pairwise interactions. Given this drastic simplification, what

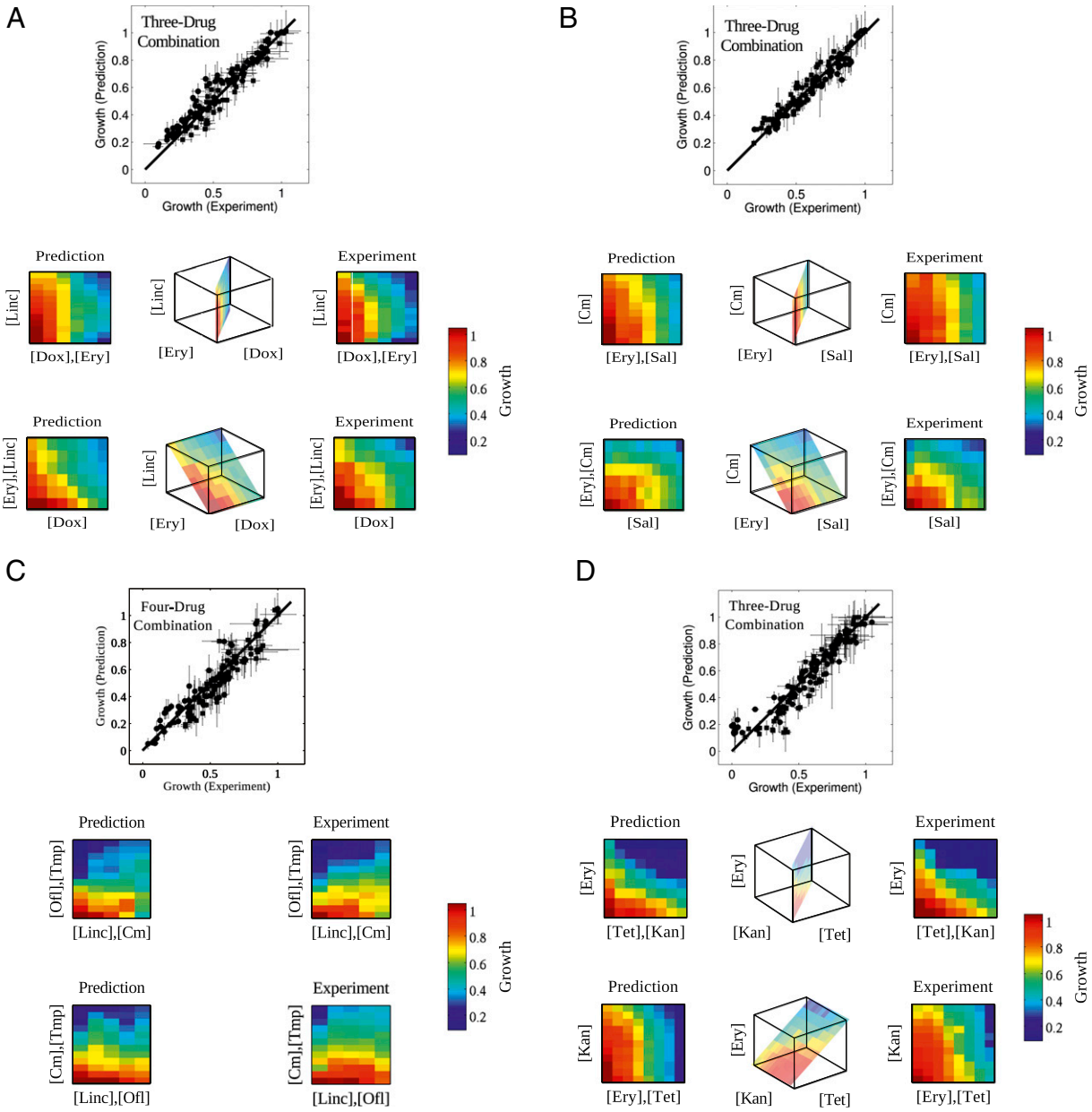

Fig. 2. Three- and four-drug interactions arise from the accumulation of pairwise interactions. Maximum entropy predictions of growth, using only data from pairwise drug interactions, match experimental growth responses in *E. coli* (*A*–*C*) and *S. aureus* (*D*) in the presence of three-drug (*A, B,* and *D*) and four-drug (*C*) combinations. In each panel, *Lower Insets* are heat maps showing the model's predictions (left) and experimental data (right) for various planes through the three- or four-dimensional spaces of drug concentrations. White squares indicate drug dosages for which the maximum entropy algorithm did not converge. Experimental error bars and 95% confidence intervals from nonlinear fitting are shown; error bars on predictions are shown, ±2 SDs of an ensemble of predictions from maximum entropy distributions calculated with random initial conditions (*SI Appendix*). Cm, chloramphenicol; Dox, doxycycline; Ery, erythromycin; Kan, kanamycin; Linc, lincomycin; Ofl, ofloxacin; Sal, salicylate; Tet, tetracycline; Tmp, trimethoprim.

outcomes are possible when drugs are combined at specific dosages? Surprisingly, there are still numerous ways that pairwise interactions can be combined to yield higher-order drug combinations (Fig. 3), even without requiring novel three-drug or four-drug effects. For example, weak synergistic interactions between drug pairs, such as those between chloramphenicol and erythromycin or erythromycin and trimethoprim, can combine to yield a cumulative effect that is strongly synergistic at particular doses (Fig. 3*A*). Conversely, as we saw, with the initial example of chloramphenicol, ofloxacin, and trimethoprim (Fig. 3*B*), that strong pairwise drug–drug interactions can combine to yield a cumulative drug effect weaker than or similar to the strongest pairwise interaction (Fig. 3*D*). In the case of salicylate, chloramphenicol, and ofloxacin, which interact antagonistically when used in pairs, the net result is an antagonistic three-drug effect whose magnitude is similar to that of the pure salicylate–ofloxacin interaction (Fig. 3*C*). In all cases, the net effect can be predicted using only the response to drug pairs (Fig. 3 *A*–*F*), illustrating that a wide range of cumulative effects are possible, depending on the dosages of each drug, even in the absence of pure three-drug or four-drug interactions. Overall, these results offer a mechanism-independent framework for predicting the cooperative effect of drug combinations on bacterial growth using only the information from the response to isolated drugs and drug pairs.

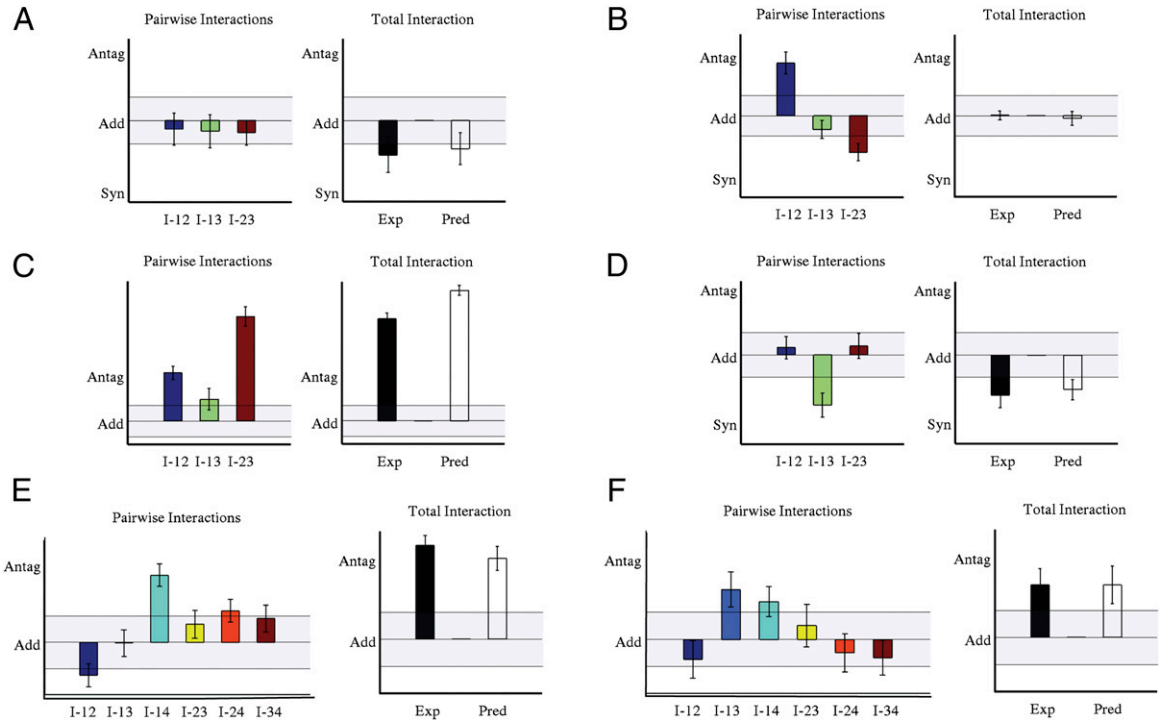

Fig. 3. Predictions highlight ways that pairwise interactions accumulate to yield higher-order interactions. Total drug interactions and pairwise drug interactions for three-drug (*A–D*) and four-drug (*E* and *F*) combinations in *E. coli* (*A–C, E,* and *F*) and *S. aureus* (*D*). Each panel shows pairwise (all panels, left, I-ij = g_{ij}-$g_i g_j$ and three-drug (*A–D,* right, g_{123}-$g_1 g_2 g_3$) or four-drug (*E* and *F,* right, g_{1234}-$g_1 g_2 g_3 g_4$) interactions at a given drug dosage. Light bars indicate maximum entropy prediction; dark bars indicate experimental result. Shaded portions of each plot indicate regions of approximately additive behavior (add, |interaction| < 0.1). In all panels, antagonism (antag) and synergy (syn) labels correspond to interactions of +0.3 and −0.3, respectively. Error bars are shown, ±SE (*SI Appendix*). Interactions that cannot be statistically explained from the pairwise predictions are less than 0.05 (units of relative growth rate) in all cases (Fig. S17). Drug combinations: A, chloramphenicol-erythromycin-trimethoprim; B, chloramphenicol-ofloxacin-trimethoprim; C, chloramphenicol-ofloxacin-salicylate; D, kanamycin-erythromycin-tetracycline; E, doxycycline-erythromycin-lincomycin-salicylate; F, chloramphenicol-ofloxacin-trimethoprim-lincomycin.

Discussion

Our experiments reveal that, for many antimicrobial drug combinations, interactions involving exactly three or more drugs do not appreciably contribute to the overall effect of the combination. The results are complementary to detailed mechanistic models because they impose an upper limit on how much mechanistic information is required to predict bacterial growth. Mechanistic and empirical approaches remain essential to characterize the effects of specific drug pairs (18–23). Remarkably, however, our results reveal that additional information is often not required to predict the effects of larger combinations of drugs. Consequently, these findings may provide a powerful strategy for the rational design of candidate therapies using combinations of three or more drugs, even when full mechanistic descriptions are not available.

Nevertheless, the approach does have practical limitations. First, the distribution $P_{pair}(x)$ (or equivalently, the single drug and two-drug effects, g_i, and g_{ij}) measured for a particular bacterial strain cannot, in general, be used to predict the multidrug response in a different strain. Using this approach to screen for multidrug combinations to combat drug-resistant mutants, for example, would require measurements of the relevant two-drug effects in each specific strain. Second, it is important to note that we chose maximum entropy as a systematic way to incorporate deviations from Bliss independence without adding spurious statistical structure. However, there may exist other pairwise models that could also be used to estimate the effects of larger drug combinations. Our primary finding is that at least one such pairwise model exists that provides excellent predictive power. Finally, one can design ad hoc examples in which any pairwise model is likely to fail. For example, if one drug were an enzyme that required two substrates, then the combination of the enzyme with both substrates might yield a completely novel three-body interaction that could not be predicted from the pairwise effects. Interestingly, however, we do not find evidence for such strong three-body interactions in any of our experiments.

Previous studies have also used pairwise approximations in other contexts, but the underlying variables represented the dynamics of specific cellular components or other physical entities such as proteins or neurons (24–30). Most notably, a recent study in cancer cells demonstrated that the expression of some proteins in response to combinations of drugs can be predicted from their responses to smaller drug combinations (24). Elucidating the biological connection between these results, at the level of individual proteins, and the integrated responses of entire cells, such as growth, remains an intriguing issue for future work. Unfortunately, fully mechanistic models of the transcriptional, metabolic, and posttranslational networks governing the multidrug response may be intractable, highlighting the need for phenomenological or statistical models to bridge this gap. To circumvent the difficulties associated with building a mechanistic model, we have formulated the problem using a mechanism-independent statistical approach. By using coarse-grained stochastic variables, X_i, whose moments $\langle X_1..X_n \rangle$ reflect the effects of a combination of N drugs, we have replaced large, intractable mechanistic models with a remarkably small statistical model of interacting drugs. Although the variables do not have a direct microscopic interpretation, they do offer a very powerful tool for inferring the relationship between the *N*-drug response and the response to drug pairs. Moreover, we find that simple formulas can yield accurate predictions as well, making the approach widely applicable and easy to implement. From a basic science perspective, the picture emerging from our analysis is surprising because it suggests that the chemical complexity underlying the cellular response to drug combinations

often does not exceed that of drug pairs. These findings therefore raise the possibility that the multidrug response in bacteria obeys statistical, rather than chemical, laws for combinations larger than two. Finally, because our findings do not depend on details of any specific cellular system, they offer a powerful predictive framework that may be applicable to other bacteria and even to eukaryotes.

Methods

Bacterial Strains. We used the WT BW25113 strain for all experiments on *E. coli* (*Δ(araD-araB)567, ΔlacZ4787(::rrnB-3), λ-, rph-1, Δ(rhaD-rhaB)568, hsdR514*) (31). We used the clinically isolated strain Newman for all experiments on *S. aureus* (32).

Drugs. We prepared all drug solutions from solid stocks (Table S1 lists drugs, their classes, and their mode of action). All antibiotic stock solutions were stored in the dark at −20 °C in single-use daily aliquots. All drugs were thawed and diluted in sterilized broth for experimental use.

Media. We used Lennox LB broth (Fisher) for experiments on *E. coli* and Tryptic Soy Broth (BD) for experiments on *S. aureus*.

Growth Conditions and Drug Treatments. For both *E. coli* and *S. aureus* experiments, we inoculated 3 mL fresh medium with a single colony and grew the cells overnight (12 h) in 14-mL culture tubes at 30 °C, with shaking at 200 rpm. Following overnight growth, stationary phase cells were diluted (5,000-fold for *E. coli*, 20,000 fold for *S. aureus*) in medium and grown for an additional 2 h at 30 °C, with shaking at 200 rpm. We then transferred 195 μL cells plus medium to 96-well plates (round-bottomed, polystyrene; Corning), and to each well we added a given combination of one, two, three, or four drugs. Specifically, we set up a 2D matrix of one-, two-, three-, or four-drug combinations, with the concentration of one or more drugs increasing along each direction of the plate. In the presence of the drugs, we grew the cells for 10–18 h at 30 °C, with shaking at 1,000 rpm on four identical vibrating plate shakers. We measured the absorbance at 600 nm (A_{600}) at time intervals dt (dt = 20 min for *E. coli*, 30 min for *S. aureus*) using a Wallac Victor-2 1420 Multilabel Counter (Perkin-Elmer) combined with an automated robotic system (Twister II, Caliper Life Sciences) to transfer plates between shakers and the reader.

Growth Rate Calculation. From the time series of A_{600}, we determined growth rates by fitting the early exponential phase portion of curves ($0.01 < A_{600} < 0.1$) to an exponential function (MATLAB 7.6.0 curve fitting toolbox, Mathworks). We normalized growth rates in the presence of single drugs (g_i) or multiple drugs (g_{ij}, g_{ijk}, g_{ijkl}) by the growth rate of cells in the absence of drugs. An example growth curve is shown in Fig. S1. SEs of the fitted growth parameter are used to estimate uncertainty in growth rates.

To minimize the small effects of day-to-day fluctuations in drug efficacy (typically <5%), we generated a standard dose–response curve (and IC_{50} value) for each drug by combining all data involving only exposure to that drug. In all subsequent three and four-drug experiments, we remeasured the IC_{50} value for each drug and scaled all concentrations to ensure that it agreed with the IC_{50} from the standard curve. Single drug (g_i) and pairwise (g_{ij}) growth rates at a given set of concentrations were then estimated by interpolating, if necessary, between data points measured at nearby concentrations.

ACKNOWLEDGMENTS. We thank C. Guet, L. Bruneaux, E. Balleza, and A. Subramaniam for technical guidance and Ilya Nemenman, Jonathon D. Shlens, Remi Monasson, Simona Cocco, Kris Wood, and all members of the Cluzel laboratory for many helpful discussions. We also thank K. Dave for editorial advice and assistance. This work was supported in part by the National Institutes of Health (NIH) Award P50GM081892-02 to the University of Chicago, AFOSR FA9550-11-1-0247 and NIH 1R01GM086881 through Rutgers University (E.D.S.), and by a National Science Foundation Postdoctoral Fellowship 0805462 (K.W.).

1. Baddour LM, et al. Committee on Rheumatic Fever, Endocarditis, and Kawasaki Disease; Council on Cardiovascular Disease in the Young; Councils on Clinical Cardiology, Stroke, and Cardiovascular Surgery and Anesthesia; American Heart Association; Infectious Diseases Society of America (2005) Infective endocarditis: Diagnosis, antimicrobial therapy, and management of complications: A statement for healthcare professionals from the Committee on Rheumatic Fever, Endocarditis, and Kawasaki Disease, Council on Cardiovascular Disease in the Young, and the Councils on Clinical Cardiology, Stroke, and Cardiovascular Surgery and Anesthesia, American Heart Association: Endorsed by the Infectious Diseases Society of America. *Circulation* 111:e394–e434.
2. Deresinski S (2009) Vancomycin in combination with other antibiotics for the treatment of serious methicillin-resistant Staphylococcus aureus infections. *Clin Infect Dis* 49:1072–1079.
3. Herbert D, et al. (1996) Bactericidal action of ofloxacin, sulbactam-ampicillin, rifampin, and isoniazid on logarithmic- and stationary-phase cultures of Mycobacterium tuberculosis. *Antimicrob Agents Chemother* 40:2296–2299.
4. Mory F, Fougnot S, Rabaud C, Schuhmacher H, Lozniewski A (2005) In vitro activities of cefotaxime, vancomycin, quinupristin/dalfopristin, linezolid and other antibiotics alone and in combination against Propionibacterium acnes isolates from central nervous system infections. *J Antimicrob Chemother* 55:265–268.
5. Bliss CI (1956) The calculation of microbial assays. *Bacteriol Rev* 20:243–258.
6. Loewe S (1953) The problem of synergism and antagonism of combined drugs. *Arzneimittelforschung* 3:285–290.
7. Greco WR, Bravo G, Parsons JC (1995) The search for synergy: A critical review from a response surface perspective. *Pharmacol Rev* 47:331–385.
8. Bollenbach T, Quan S, Chait R, Kishony R (2009) Nonoptimal microbial response to antibiotics underlies suppressive drug interactions. *Cell* 139:707–718.
9. Huovinen P, Wolfson JS, Hooper DC (1992) Synergism of trimethoprim and ciprofloxacin in vitro against clinical bacterial isolates. *Eur J Clin Microbiol Infect Dis* 11:255–257.
10. Cover TM, Thomas JA (2006) *Elements of Information Theory, XXIII* (Wiley-Interscience, Hoboken, NJ).
11. Jaynes ET (1957) Information theory and statistical mechanics. *Phys Rev* 106:620–630.
12. Isserlis L (1918) On a formula for the product-moment coefficient of any order of a normal frequency distribution in any number of variables. *Biometrika* 12:134–139.
13. Langlois R, Cantor CR, Vince R, Pestka S (1977) Interaction between the erythromycin and chloramphenicol binding sites on the Escherichica coli ribosome. *Biochemistry* 16:2349–2356.
14. Cohen SP, Levy SB, Foulds J, Rosner JL (1993) Salicylate induction of antibiotic resistance in Escherichia coli: Activation of the mar operon and a mar-independent pathway. *J Bacteriol* 175:7856–7862.
15. Haight TH, Finland M (1952) Laboratory and clinical studies on erythromycin. *N Engl J Med* 247:227–232.
16. Amari S (2001) Information geometry on hierarchy of probability distributions. *IEEE Trans Inf Theory* 47:1701–1711.
17. Schneidman E, Still S, Berry MJ, 2nd, Bialek W (2003) Network information and connected correlations. *Phys Rev Lett* 91:238701.
18. Fitzgerald JB, Schoeberl B, Nielsen UB, Sorger PK (2006) Systems biology and combination therapy in the quest for clinical efficacy. *Nat Chem Biol* 2:458–466.
19. Jonker DM, Visser SAG, van der Graaf PH, Voskuyl RA, Danhof M (2005) Towards a mechanism-based analysis of pharmacodynamic drug-drug interactions in vivo. *Pharmacol Ther* 106:1–18.
20. Keith CT, Borisy AA, Stockwell BR (2005) Multicomponent therapeutics for networked systems. *Nat Rev Drug Discov* 4:71–78.
21. Kohanski MA, Dwyer DJ, Collins JJ (2010) How antibiotics kill bacteria: From targets to networks. *Nat Rev Microbiol* 8:423–435.
22. Lehár J, Stockwell BR, Giaever G, Nislow C (2008) Combination chemical genetics. *Nat Chem Biol* 4:674–681.
23. Lehár J, et al. (2007) Chemical combination effects predict connectivity in biological systems. *Mol Syst Biol* 3:80.
24. Geva-Zatorsky N, et al. (2010) Protein dynamics in drug combinations: A linear superposition of individual-drug responses. *Cell* 140:643–651.
25. Margolin AA, et al. (2006) ARACNE: An algorithm for the reconstruction of gene regulatory networks in a mammalian cellular context. *BMC Bioinformatics* 7 (Suppl 1):S7.
26. Mora T, Walczak AM, Bialek W, Callan CG, Jr. (2010) Maximum entropy models for antibody diversity. *Proc Natl Acad Sci USA* 107:5405–5410.
27. Shlens J, et al. (2009) The structure of large-scale synchronized firing in primate retina. *J Neurosci* 29:5022–5031.
28. Shlens J, et al. (2006) The structure of multi-neuron firing patterns in primate retina. *J Neurosci* 26:8254–8266.
29. Schneidman E, Berry MJ, 2nd, Segev R, Bialek W (2006) Weak pairwise correlations imply strongly correlated network states in a neural population. *Nature* 440:1007–1012.
30. Chatterjee MS, Purvis JE, Brass LF, Diamond SL (2010) Pairwise agonist scanning predicts cellular signaling responses to combinatorial stimuli. *Nat Biotechnol* 28:727–732.
31. Baba T, et al. (2006) Construction of Escherichia coli K-12 in-frame, single-gene knockout mutants: The Keio collection. *Mol Syst Biol* 2:2006–2008.
32. Baba T, Bae T, Schneewind O, Takeuchi F, Hiramatsu K (2008) Genome sequence of Staphylococcus aureus strain Newman and comparative analysis of staphylococcal genomes: Polymorphism and evolution of two major pathogenicity islands. *J Bacteriol* 190:300–310.

Supporting Information Appendix

Contents

Table S1: Drug List and Abbreviations

Drug (Abbreviation, Source)	**Class**	**Mode of Action**
Chloramphenicol (Cm, chloramphenicol, MP biomedicals)	Protein synthesis inhibitor (50 S target)	Inhibits peptidyl transferase activity
Doxycycline (Doxy, doxycycline hyclate, Sigma Aldrich)	Protein synthesis inhibitor (30 S target)	Inhibits binding of aminoacyl t-RNA
Erythromycin (Ery, erythromycin, Sigma Aldrich)	Protein synthesis inhibitor (macrolide)	Inhibits translocation of peptidyl t-RNA
Lincomycin (Linc, lincomycin hydrochloride, MP biomedicals)	Protein synthesis inhibitor (50 S target)	Inhibits peptidyl transferase activity
Ciprofloxacin (Cip, ciprofloxacin, Sigma Aldrich)	DNA synthesis inhibitor (fluoroquinolone)	Inhibits activity of DNA gyrase
Ofloxacin (Ofl, ofloxacin, Sigma Aldrich)	DNA synthesis inhibitor (fluoroquinolone)	Inhibits activity of DNA gyrase
Trimethoprim (Tmp, trimethoprim, Sigma Aldrich)	Folic acid synthesis inhibitor	Inhibits dihydrofolate reductase
Salicylate (Sal, sodium salicylate, Sigma Aldrich)	Pain reliever	Inducer of mar system
Tetracycline (Tet, tetracycline hydrochloride, Acros)	Protein synthesis inhibitor (30 S target)	Inhibits binding of aminoacyl t-RNA
Kanamycin (Kan, kanamycin monosulfate, Fisher)	Aminoglycoside	Stalls 30S initiation complex; induces misreading of mRNA
Tobramycin (Tobr, tobramycin, TCI)	Aminoglycoside	Binds to 30S and 50S ribosomes,
Penicillin G (PenG, penicillin G potassium, Fisher)	Cell wall synthesis inhibitor	Inhibits peptidoglycan cross-linking
Ampicillin (Amp, ampicillin sodium salt , Fisher)	Cell wall synthesis inhibitor	Inhibits peptidoglycan cross-linking
Sodium Benzoate (NaBenz, sodium benzoate, Sigma Aldrich)	Preservative	Inducer of mar system
Bacitracin (Bac, bacitracin, USB)	Polypeptide antibiotic	Interferes with cell wall construction
Sulfamonomethoxine (Sulf, sulfamonomethoxine, TCI)	Folic acid synthesis inhibitor	Inhibits PABA dihydrofolate synthase
Spectinomycin (Spect, spectinomycin dihydrochloride, Sigma Aldrich)	Protein synthesis inhibitor (aminocyclitol)	Stalls 30S initiation complex
Spiramycin (Spir, spiramycin, TCI)	Protein synthesis inhibitor (macrolide)	Inhibits translocation of peptidyl t-RNA
Naladixic Acid (Nal Acid, naladixic acid, Fisher)	DNA synthesis inhibitor (quinolone)	Inhibits activity of DNA gyrase

Table S2:

Drug Combination	R^2 (Pairwise)	R^2 (Independent)	ΔAIC	Weight for Pairwise
Sal-Ery-Cm	0.93	0.82	-109.0	> 0.999
Cm-Ery-Tmp	0.87	0.87	-5.9	0.95
Cm-Ofl-Sal	0.74	**	-909.4	> 0.999
Cm-Ofl-Tmp	0.90	0.87	-14.4	> 0.999
Dox-Ery-Linc	0.86	0.88	51.5	< 0.001
Dox-Ery-Linc-Sal	0.72	**	-161.6	> 0.999
Linc-Cm-Ofl-Tmp	0.85	0.70	-83.4	> 0.999
All Data	**0.90**	**0.33**	**-2233.2**	**> 0.999**

Table S2. Comparison of Pairwise Approximation with Independent Model
Coefficient of determination, R^2, is defined as $R^2 = 1\text{-}SS_{err} / SS_{tot}$, where SS_{err} is the residual sum of squares between model and data, and SS_{tot} is the total sum of squares (proportional to the variance of the experimental measurements). ΔAIC is the difference in AIC values between the pairwise and the independent model. The last column provides the Akaike weight in favor of the pairwise model. Drug abbreviations are given in Table S1.

** $R^2<0$, which indicates very poor fit (the mean of the data provides a better fit than the model)

Table S3: Drug Combinations Used in Combinatorial Experiments:

Total of 120 unique drug dosage combinations comprised of 93 unique 3-drug combinations. Note that some of the 3-drug combinations (e.g. ampicillin, spectinomycin, and spiramycin) are repeated at different dosages.

**Drug concentrations are given in ug/mL with the following exceptions: [Cip] is ng/mL, [Sal] is mM, and [NaBenz] is mM.

Abbreviations: Amp is ampicillin, Cip is ciprofloxacin, Tobr is tobramycin, Nal Acid is naladixic acid, Spect is spectinomycin, Spir is spiramycin, NaBenz is sodium benzoate, Tmp is trimethoprim, Sulf is sulfamonomethexate, Dox is doxyclycine, Cm is chloramphenicol, PenG is penicillin G, and Bac is bacitracin.

Label	Drug 1	[Drug 1] (ug/mL)**	Drug 2	[Drug 2] (ug/mL)**	Drug 3	[Drug 3] (ug/mL)**
	Combinatorial Experiment 1 (7 drugs): Amp, Cip, Tobr, Tmp, Nal Acid, Spect, Spir					
1	Amp	1.5	Cip	3	Tobr	1.6
2	Amp	1.5	Cip	3	Tmp	0.15
3	Amp	1.5	Cip	3	Nal Acid	1.75
4	Amp	1.5	Cip	3	Spect	10
5	Amp	1.5	Cip	3	Spir	200
6	Amp	1.5	Tobr	1.6	Tmp	0.15
7	Amp	1.5	Tobr	1.6	Nal Acid	1.75
8	Amp	1.5	Tobr	1.6	Spect	10
9	Amp	1.5	Tobr	1.6	Spir	200
10	Amp	1.5	Tmp	0.15	Nal Acid	1.75
11	Amp	1.5	Tmp	0.15	Spect	10
12	Amp	1.5	Tmp	0.15	Spir	200
13	Amp	1.5	Nal Acid	1.75	Spect	10
14	Amp	1.5	Nal Acid	1.75	Spir	200
15	Amp	1.5	Spect	10	Spir	200
16	Cip	3	Tobr	1.6	Tmp	0.15
17	Cip	3	Tobr	1.6	Nal Acid	1.75
18	Cip	3	Tobr	1.6	Spect	10
19	Cip	3	Tobr	1.6	Spir	200
20	Cip	3	Tmp	0.15	Nal Acid	1.75
21	Cip	3	Tmp	0.15	Spect	10
22	Cip	3	Tmp	0.15	Spir	200
23	Cip	3	Nal Acid	1.75	Spect	10
24	Cip	3	Nal Acid	1.75	Spir	200
25	Cip	3	Spec	10	Spir	200
26	Tobr	1.6	Tmp	0.15	Nal Acid	1.75
27	Tobr	1.6	Tmp	0.15	Spect	10

Label	Drug 1	[Drug 1] (ug/mL)**	Drug 2	[Drug 2] (ug/mL)**	Drug 3	[Drug 3] (ug/mL)**
28	Tobr	1.6	Tmp	0.15	Spir	200
29	Tobr	1.6	Nal Acid	1.75	Spect	10
30	Tobr	1.6	Nal Acid	1.75	Spir	200
31	Tobr	1.6	Spect	10	Spir	200
32	Tmp	0.15	Nal Acid	1.75	Spect	10
33	Tmp	0.15	Nal Acid	1.75	Spir	200
34	Tmp	0.15	Spect	10	Spir	200
35	Nal Acid	1.75	Spect	10	Spir	200
Combinatorial Experiment 2 (6 drugs): Amp, NaBenz, Tmp, Nal Acid, Spect, Spir						
36	Amp	0.9	NaBenz	2	Tmp	0.05
37	Amp	0.9	NaBenz	2	Nal Acid	1.25
38	Amp	0.9	NaBenz	2	Spect	9
39	Amp	0.9	NaBenz	2	Spir	200
40	Amp	0.9	Tmp	0.05	Nal Acid	1.25
41	Amp	0.9	Tmp	0.05	Spect	9
42	Amp	0.9	Tmp	0.05	Spir	200
43	Amp	0.9	Nal Acid	1.25	Spect	9
44	Amp	0.9	Nal Acid	1.25	Spir	200
45	Amp	0.9	Spect	9	Spir	200
46	NaBenz	2	Tmp	0.05	Nal Acid	1.25
47	NaBenz	2	Tmp	0.05	Spect	9
48	NaBenz	2	Tmp	0.05	Spir	200
49	NaBenz	2	Nal Acid	1.25	Spect	9
50	NaBenz	2	Nal Acid	1.25	Spir	200
51	NaBenz	2	Spect	9	Spir	200
52	Tmp	0.05	Nal Acid	1.25	Spect	9
53	Tmp	0.05	Nal Acid	1.25	Spir	200
54	Tmp	0.05	Spect	9	Spir	200
55	Nal Acid	1.25	Spect	9	Spir	200
Combinatorial Experiment 3 (5 drugs): Amp, Tobr, Nal Acid, Spect, Spir						
56	Amp	0.8	Tobr	1.6	Nal Acid	1
57	Amp	0.8	Tobr	1.6	Spect	8
58	Amp	0.8	Tobr	1.6	Spir	200
59	Amp	0.8	Nal Acid	1	Spect	8
60	Amp	0.8	Nal Acid	1	Spir	200
61	Amp	0.8	Spect	8	Spir	200
62	Tobr	1.6	Nal Acid	1	Spect	8
63	Tobr	1.6	Nal Acid	1	Spir	200

Label	Drug 1	[Drug 1] (ug/mL)**	Drug 2	[Drug 2] (ug/mL)**	Drug 3	[Drug 3] (ug/mL)**
64	Tobr	1.6	Spect	8	Spir	200
65	Nal Acid	1	Spect	8	Spir	200
Combinatorial Experiment 4 (7 drugs): Amp, Cip, Sulf, Tmp, NaBenz, Dox, Cm						
66	Amp	1.25	Cip	3.5	Sulf	1.5
67	Amp	1.25	Cip	3.5	Tmp	0.13
68	Amp	1.25	Cip	3.5	NaBenz	1.5
69	Amp	1.25	Cip	3.5	Dox	0.15
70	Amp	1.25	Cip	3.5	Cm	0.5
71	Amp	1.25	Sulf	1.5	Tmp	0.13
72	Amp	1.25	Sulf	1.5	NaBenz	1.5
73	Amp	1.25	Sulf	1.5	Dox	0.15
74	Amp	1.25	Sulf	1.5	Cm	0.5
75	Amp	1.25	Tmp	0.13	NaBenz	1.5
76	Amp	1.25	Tmp	0.13	Dox	0.15
77	Amp	1.25	Tmp	0.13	Cm	0.5
78	Amp	1.25	NaBenz	1.5	Dox	0.15
79	Amp	1.25	NaBenz	1.5	Cm	0.5
80	Amp	1.25	Dox	0.15	Cm	0.5
81	Cip	3.5	Sulf	1.5	Tmp	0.13
82	Cip	3.5	Sulf	1.5	NaBenz	1.5
83	Cip	3.5	Sulf	1.5	Dox	0.15
84	Cip	3.5	Sulf	1.5	Cm	0.5
85	Cip	3.5	Tmp	0.13	NaBenz	1.5
86	Cip	3.5	Tmp	0.13	Dox	0.15
87	Cip	3.5	Tmp	0.13	Cm	0.5
88	Cip	3.5	NaBenz	1.5	Dox	0.15
89	Cip	3.5	NaBenz	1.5	Cm	0.5
90	Cip	3.5	Dox	0.15	Cm	0.5
91	Sulf	1.5	Tmp	0.13	NaBenz	1.5
92	Sulf	1.5	Tmp	0.13	Dox	0.15
93	Sulf	1.5	Tmp	0.13	Cm	0.5
94	Sulf	1.5	NaBenz	1.5	Dox	0.15
95	Sulf	1.5	NaBenz	1.5	Cm	0.5
96	Sulf	1.5	Dox	0.15	Cm	0.5
97	Tmp	0.13	NaBenz	1.5	Dox	0.15
98	Tmp	0.13	NaBenz	1.5	Cm	0.5
99	Tmp	0.13	Dox	0.15	Cm	0.5
100	NaBenz	1.5	Dox	0.15	Cm	0.5

Label	Drug 1	[Drug 1] (ug/mL)**	Drug 2	[Drug 2] (ug/mL)**	Drug 3	[Drug 3] (ug/mL)**
Combinatorial Experiment 5 (6 drugs): PenG, Bac, Sulf, Dox, Cip, Cm						
101	PenG	20	Bac	200	Sulf	2.5
102	PenG	20	Bac	200	Dox	0.25
103	PenG	20	Bac	200	Cip	5
104	PenG	20	Bac	200	Cm	0.4
105	PenG	20	Sulf	2.5	Dox	0.25
106	PenG	20	Sulf	2.5	Cip	5
107	PenG	20	Sulf	2.5	Cm	0.4
108	PenG	20	Dox	0.25	Cip	5
109	PenG	20	Dox	0.25	Cm	0.4
110	PenG	20	Cip	5	Cm	0.4
111	Bac	200	Sulf	2.5	Dox	0.25
112	Bac	200	Sulf	2.5	Cip	5
113	Bac	200	Sulf	2.5	Cm	0.4
114	Bac	200	Dox	0.25	Cip	5
115	Bac	200	Dox	0.25	Cm	0.4
116	Bac	200	Cip	5	Cm	0.4
117	Sulf	2.5	Dox	0.25	Cip	5
118	Sulf	2.5	Dox	0.25	Cm	0.4
119	Sulf	0.25	Cip	5	Cm	0.4
120	Dox	0.25	Cip	5	Cm	0.4

Table S4:

Drug Combination	f_c
E. coli	
Sal-Ery-Cm	0.95
Cm-Ery-Tmp	0.89
Cm-Ofl-Sal	0.98
Cm-Ofl-Tmp	0.95
Dox-Ery-Linc	0.94
S. aureus	
Tet-Kan-Ery	0.93
Total (All Drugs)	**0.97**

Table S4. Validation of Pairwise Approximation. f_c represents the fraction of total three-drug correlations that are captured by the pairwise model. For each drug dosage containing nonzero amounts of all three drugs, we calculated the maximum entropy distributions P_N (N=1,2,3), which are consistent with all measurements involving N or fewer drugs. We then calculated the multi-information $I_3 = S_1 - S_3$, where S_i is the entropy of the distribution P_i. The fraction of total correlations captured by the pairwise model is then

$$f_c = \frac{\sum I_2}{\sum I_3}$$

where sums run over all data points for a given 3-drug combination. An f_c of 1 would indicate that the pairwise model captured all higher-order correlations or, equivalently, that interactions involving exactly N drugs (for N>2) do not contribute to the multi-drug effects. Cm, chloramphenicol; Dox, doxycycline; Ery, erythromycin; Kan, kanamycin; Linc, lincomycin; Ofl, ofloxacin; Sal, salicylate . Tet, tetracycline; Tmp, trimethoprim.

2 Supporting Text

2.1 Example Growth Curve

An example growth curve is shown in Figure S1.

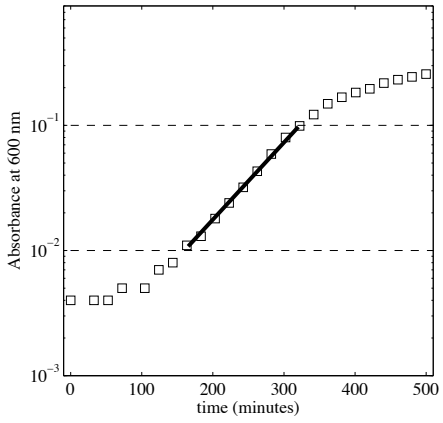

Figure S1: Growth Rate Measurement. Time series of A_{600} vs. time. Solid line, fit to exponential function. Dashed lines, region of exponential growth. Growth rate is given by the slope of the line.

2.2 Statistical Framework for Drug Combinations

The ultimate goal of our analysis is to establish a predictive relationship between the effects of small drug combinations (1- or 2-drug combinations) and the effects of larger multi-drug combinations. Because mechanistic models for large intracellular networks are often not tractable, we introduce a statistical framework which, by construction, associates drug interactions to correlations between stochastic variables. The model offers one way of establishing testable predictions by first mapping experimental measurements to moments of a joint probability distribution. The problem is then reduced to estimating the unknown distribution, which can be achieved using statistical techniques, such as entropy maximization, or (in principle) by incorporating other assumptions about the underlying physical system.

Specifically, we assume that interactions between N drugs can be modeled as correlations between N continuous stochastic variables, $X_i, (i = 1...N)$, such

that the observed growth of cells ($g_{1,2..N}$) in the presence of N drugs is given by

$$g_{1,2..N} = \langle X_1 X_2 ... X_N \rangle \tag{S1}$$

where brackets represent an expectation value over an ensemble described by the unknown probability density $P(x_1, x_2, ...x_N)$. If the variables X_i are uncorrelated, the growth reduces to a product

$$g_{1,2..N} = \langle X_1 \rangle \langle X_2 \rangle ... \langle X_N \rangle \equiv g_1 g_2 ... g_N, \tag{S2}$$

which is equivalent to Bliss independence, a common phenomenological model used in pharmacology to describe non-interacting drugs [2].

We would like to ask whether pairwise interactions between drugs can be used to predict the effects of larger combinations of drugs. Within the above framework, predicting effects of drug combinations reduces to estimating moments of the unknown distribution $P(x_1, x_2, ...x_N)$ using data on interactions between pairs of drugs. Therefore, to test our hypothesis, we must estimate higher-order moments of $P(x_1, x_2, ...x_N)$ (the effects of a multi-drug combination) using only the lower order moments (the effects of two-drug combinations). The question, then, is how does one estimate, without mechanistic assumptions or a physical model, the unknown probability distribution $P(x_1, x_2, ...x_N)$ given only information about some collection of moments of that distribution,

$$\langle f_j \rangle \equiv \int_a^b \int_a^b ... \int_a^b P(x_1, x_2, ...x_N) f_j(x_1, x_2, ...x_N) dx_1 dx_2 ... dx_N = \alpha_j. \tag{S3}$$

Entropy maximization offers one method of solving this problem by choosing a distribution consistent with known moments but that does not incorporate additional statistical structure [18, 19, 33].

In what follows, we restrict ourselves for illustrative purposes to the three-drug case, though the results are easily generalizable to any larger drug combination. To estimate $P(x_1, x_2, x_3)$, we maximize the entropy, $S(P)$, subject to the known moment constrains. The entropy, $S(P)$, is defined (up to an additive constant) as

$$S(P) = -\int_a^b \int_a^b \int_a^b P(x_1, x_2, x_3) \log \left(\frac{P(x_1, x_2, x_3)}{q(x_1, x_2, x_3)} \right) dx_1 dx_2 dx_3, \tag{S4}$$

where $q(x_1, x_2, x_3)$ is a continuous prior distribution that accounts for an a priori knowledge gleaned from, for example, physical considerations or experience. The maximization amounts to minimizing the Kullback-Leibler divergence [35] between the distributions P and q, subject to constraints on the moments. We choose the interval $[a, b]$ to be finite and take $q(x_1, x_2, x_3)$ to be a constant, which is equivalent to assuming a uniform prior distribution. We stress that our results do not depend on a specific choice of $[a, b]$, as long as some minimal conditions are met (see below).

To proceed with the estimation of $P(x_1, x_2, x_3)$, we first measured the growth response to each drug i alone (g_i) and to all pairs of drugs, (g_{ij}). To predict the

effects of a given three-drug combination, for example, we measured g_1, g_2, g_3, g_{12}, g_{13}, and g_{23}. The corresponding constraints on the distribution are simply

$$\begin{aligned}
\langle f_1 \rangle &\equiv \int_a^b \int_a^b \int_a^b P(x_1, x_2, x_3) x_1 dx_1 dx_2 dx_3 = g_1, \\
\langle f_2 \rangle &\equiv \int_a^b \int_a^b \int_a^b P(x_1, x_2, x_3) x_2 dx_1 dx_2 dx_3 = g_2, \\
\langle f_3 \rangle &\equiv \int_a^b \int_a^b \int_a^b P(x_1, x_2, x_3) x_3 dx_1 dx_2 dx_3 = g_3, \\
\langle f_4 \rangle &\equiv \int_a^b \int_a^b \int_a^b P(x_1, x_2, x_3) x_1 x_2 dx_1 dx_2 dx_3 = g_{12}, \\
\langle f_5 \rangle &\equiv \int_a^b \int_a^b \int_a^b P(x_1, x_2, x_3) x_1 x_3 dx_1 dx_2 dx_3 = g_{13}, \\
\langle f_6 \rangle &\equiv \int_a^b \int_a^b \int_a^b P(x_1, x_2, x_3) x_2 x_3 dx_1 dx_2 dx_3 = g_{23}.
\end{aligned} \tag{S5}$$

We can use Lagrange multipliers $(\lambda_0, h_1, h_2, h_3, J_{12}, J_{13}, J_{23})$ to maximize the entropy $S(P)$ subject to these constraints, which leads to

$$P(x_1, x_2, x_3) = \frac{1}{Z} \exp\left(h_1 x_1 + h_2 x_2 + h_3 x_3 + J_{12} x_1 x_2 + J_{13} x_1 x_3 + J_{23} x_2 x_3\right), \tag{S6}$$

where Z is a constant (related to λ_0) that normalizes the distribution. It can be shown that, in general, the entropy of a distribution calculated in this way corresponds to the global maximum, if it exists [19],[33].

We have labeled the Lagrange multipliers as h_i and J_{ij} in accordance with notation commonly used for the well-known Ising model, which takes a similar form [36]. In the context of our drug interaction model, h_i encodes the single-drug growth response and J_{ij} encodes information about deviations from Bliss independence for a given drug pair, with $J_{ij} > 0$ indicating antagonism and $J_{ij} < 0$ indicating synergy. We call the parameter h_i the resilience coefficient and J_{ij} the drug-drug coupling coefficient between the drugs i and j; they characterize the response to single drugs and to pairs of drugs, respectively (Fig. S2). Intuitively, the value of the resilience coefficient reflects the cell growth in response to a given concentration of one drug (Fig. S2). The resilience coefficient decreases with increasing drug concentration. The drug-drug coupling coefficient, J, reflects, for each drug dosage, the nature of interactions taking place between two given drugs (Fig. S2). For example, when J is zero, there exists no drug-drug coupling and the two drugs act independently. When J is positive, the drug pair is antagonistic and for negative values, the pair is synergistic.

2.2.1 Growth Rate Predictions and Uncertainties

In practice, we calculate the parameters h_i and J_{ij} from experimental data using a standard numerical technique that involves minimizing a dual space

Lagrangian [37]. The minimization occurs on a convex surface and can be accomplished with any unconstrained optimization algorithm. For each dosage of a given three- or four-drug combination, we performed the optimization 50 times (for 3 drugs) or 25 times (for four drugs) starting from random initial conditions drawn from a uniform distribution on the interval $[-0.5, 0.5]$. Nonphysical predictions ($g < 0$, $g > 1$) occasionally arise from strongly synergistic or strongly antagonistic combinations, and these are set to 0 (no growth) or 1 (maximum growth), respectively. While the minimization should not be prone to errors due to local minima, we find that fits of similar quality can be achieved using a range of parameter values; hence, there is some uncertainty in the location of the true minimum. Taking random initial conditions allows us to estimate this uncertainty and offer more reliable predictions. All predictions represent the mean of these trials. Error bars of the growth predictions in Figure 2 are $\pm 2\sigma$, with σ the standard deviation of the distribution of trials. Standard errors of the mean, which are between 5 and 8 times smaller, could be used instead to give a true estimate of the error associated with each prediction, but they leave the reader without a sense of σ. Uncertainties in the prediction of drug interactions, $I_{1..N} \equiv g_{12..N} - g_1 g_2 ... g_N$, (Figure 3) must incorporate standard errors from single drug measurements (g_i). Therefore, the error bars represent $\pm$ 1 standard error of the mean. For distributions of 25 or 50 trials, the standard error associated with the prediction of the first term ($g_{12..N}$) is much smaller than that of the second term ($g_1 g_2 ... g_N$). Uncertainties of the drug interaction predictions are therefore dominated by standard errors in the estimates of single drug growth rates g_i appearing in the second term.

2.2.2 Choosing the State Space

The calculation of the maximum entropy distribution requires a specific choice of state space, $[a, b]$, for each continuous stochastic variable X_i. First, we note that if the boundaries are chosen such that $[a, b] = [-\infty, \infty]$ - that is, the variables take values on the real line - a (normalizable) distribution of the form Equation S6 does not exist, because there are no constraints on the variances, $\langle X_i^2 \rangle$. In practice, this difficulty can be circumvented by choosing $[a, b]$ to be finite, which puts implicit limits on the variance of each variable. While this amounts to an additional assumption, we find empirically that the predictions of higher moments from lower moments do not depend on the choice $[a, b]$ as long as i) the distribution of the form Equation S6 is normalizable and ii) a solution to Equations S5, S6 can be found for some choice of Lagrange multipliers. The specific values of the Lagrange multipliers will of course depend on the choice of state space, but the relationship between higher moments and lower moments conforms to that given by Issesrlis' theorem in all cases where a suitable solution to Equation 5 is found. We return to this point below.

Figures S3, S4 illustrate the fit of models with different choices of (a, b) to all two-drug and single drug data. We note that these are not predictions, but simply fits to examine whether a solution to Equations S5, S6 can be found. Figure S3 illustrates that choices with $(a, b) = (0, b)$ for $b > 0$ do not provide

an accurate description of many of the measured drug interactions; that is, a valid solution cannot be found. On the other hand, the fit improves significantly when $a < 0$ and $b > 0$ (Figure S4). For sufficiently large $|b - a|$, the fit again becomes poor, likely because of the failure of numerical integration over the increasingly large state space. Hence, for all three-drug calculations, we choose $(a, b) = (-3, 4)$ (Figure S4, lower left panel), which provides an excellent fit ($R^2 > 0.99$) to the pairwise data, indicating that a solution to Equations S5, S6 is achievable. This choice is not unique, and other choices (e.g. $(a, b) = (-9, 10)$) are possible but must utilize more computational resources to calculate integrals at the same level of accuracy. For similar reasons, we choose a smaller range $(a, b) = (-1, 2)$ for four-drug predictions to allow for faster computation of the numerical integrals. The final predictions do not depend on these choices of state space, but instead only on the measured growth rates for drug pairs and single drugs. The exact same results are also obtained if we choose the variables to be discrete "spin-like" variables, as long as the value of the spin is sufficiently large (e.g. spin $= \pm 4$). In the latter case, the integrals become sums that are easily calculated.

2.2.3 Example Maximum Entropy Distributions

We illustrate example (marginal) maximum entropy distributions calculated for the drug combination salicylate, erythromycin, and chloramphenicol in Figures S5, S6. Figure S5 shows the pairwise, $P_2(x_1, x_2) \equiv \int_a^b P(x_1, x_2, x_3)dx_3$, and single variable, $P_1(x_1) \equiv \int_a^b P(x_1, x_2, x_3)dx_3dx_2$, marginal distributions for the three-drug combination at a given dose of each drug. In this figure, the concentration of chloramphenicol is 0, so these distributions describe the effects of salicylate and erythromycin alone (right panels) and in combination (left panel). Similarly, Figure S6 shows the pairwise and single variable marginal distributions for erythromycin and chloramphenicol in the absence of salicylate. Deviations from the uniform distribution ensure that the experimental measurements of pairwise drug interactions (2-body correlations) and single-drug effects (single variable means) are appropriately described by expectation values of P.

2.2.4 Isserlis' Theorem Describes Observed Moment Relationships

Empirically, we find that the moment relationships derived from our experiments are consistent with the well-known Isserlis' formula [38],

$$\langle X_i X_j X_k \rangle = \langle X_i \rangle \langle X_j X_k \rangle + \langle X_j \rangle \langle X_i X_k \rangle + \langle X_k \rangle \langle X_i X_j \rangle - 2\langle X_i \rangle \langle X_j \rangle \langle X_k \rangle, \quad \text{(S7)}$$

or in terms of the growth measurements,

$$g_{ijk} = g_i g_{jk} + g_j g_{ik} + g_k g_{ij} - 2 g_i g_j g_k. \quad \text{(S8)}$$

Similar expressions hold for higher order moments. For example,

$$g_{ijkl} = g_{il} g_{jk} + g_{ik} g_{jl} + g_{ij} g_{kl} - 2 g_i g_j g_k g_l. \quad \text{(S9)}$$

Isserlis' equations were originally proven for jointly distributed Gaussian variables, but they have also been extended to certain classes of non-Gaussian variables [39]. These relationships can be derived from the maximum entropy results using first order perturbation theory when the drug-drug coupling is small compared to the single drug effects; they are exact if the distribution $P(x)$ is Gaussian. The result (Figure S7) is perhaps not surprising, given that the choice of finite $[a, b]$ implicitly constrains the variance of the distributions.

Consider, for example, that the same relationship can also be achieved in the following way. Assume that the variables are constrained such that $\langle X_i^2 \rangle = \sigma_i^2$ for some choice of constants $\sigma_i^2 > 0$. Under these conditions, the maximum entropy distribution for variables defined on the real line is a Gaussian [33]. Therefore, Isserlis' theorem will describe the moment relationships, and the result will not depend on the specific choices of σ_i^2, as long as they are sufficiently large that a distribution satisfying all moment constraints exists.

The success of Equation S8 and, more generally, Isserlis' theorem in predicting the effects of large drug combinations is, in itself, a striking result. It suggests that one could arrive at the same predictions by assuming, at the outset, that the variables X_i come from a multi-variate Gaussian distribution. Such a relationship could arise, for example, from the Central Limit Theorem if one could argue that the underlying stochasticity of intracellular networks contributing to the multi-drug response arises from a sum of independent, or nearly independent, stochastic variables. This remains an open question for future work. Nevertheless, in practice, the simplicity of the algebraic expressions given by Isserlis renders the method useful even to those without extensive computational resources or experience.

2.2.5 Drug With Itself

In pharmacology, Bliss independence is well-known to be a poor model for the effects of a two drugs with highly similar mechanisms. In particular, it is often noted that Bliss independence cannot accurately describe an experiment where a drug is divided into two volumes which are then combined (i.e. the "interactions" of a drug with itself). Our results extend Bliss independence to account for interactions between drug pairs, which raises the question of whether the model can more accurately describe the "interaction" of a drug with itself. Applying equation 8 to a such a scenario, we have

$$\begin{aligned} g(c_1 + c_2 + c_3) =& g(c_1)g(c_2 + c_3) + g(c_2)g(c_1 + c_3) + \\ & g(c_3)g(c_1 + c_2) - 2g(c_1)g(c_2)g(c_3), \end{aligned} \tag{S10}$$

where $g(x)$ is the growth in the presence of a drug at a concentration x. One solution to this equation is given by an exponential function, which is a reasonable model for the dose-response curve of many drugs over limited concentration ranges. However, dose-response curves are typically modeled with a Hill function, $g(x) = (1 + (x/K)^n)^{-1}$, which is consistent with our single-drug data but is not a solution of equation S10. To explore the usefulness of equation S10 for

describing typical Hill-like dose-response relationships, we consider Hill functions with Hill coefficients of $n = 1$, $n = 2$, and $n = 5$ (and $K = 1$ without loss of generality). We then compare the predictions of equation S10 and the predictions of Bliss independence (given by $g(c_1 + c_2 + c_3) = g(c_1)g(c_2)g(c_3)$) with the true Hill function (Figure S8). The pairwise model significantly improves upon Bliss independence, especially when Hill coefficients are near 1, but it can not perfectly capture steep features of the dose-response curve for larger n and high drug dosages. These results suggest that the model may lose accuracy at high dosages when drug combinations involve drugs with identical mechanisms of action and steep dose-response curves. In practice, we find that dose response curves rarely have $n > 2$, and furthermore, the method works well even when drugs have similar–but not identical–modes of action (See Dox-Ery-Linc combo in main text, Figure 2). Therefore, this theoretical limitation is unlikely to be relevant in most practical situations.

2.3 Failure and Success of Bliss Independent Model

While our pairwise model performs significantly better, on the whole, than the Bliss independent model, we found that some combinations of three drugs may nevertheless be appropriately modeled with Bliss independence. Figure S9 compares predictions from Bliss independence (left) with those from the pairwise model (right) for two 3-drug combinations. In the top drug combination (Cm-Ofl-Sal), the pairwise approximation significantly outperforms the independent model. On the other hand, in the lower panels (Dox-Ery-Linc), the results from both models are highly correlated ($r \approx 0.95$) and both provide reasonable fits to the data. The latter result is particularly interesting given the strong interactions that take place between doxycycline-lincomycin (strong suppression) and doxycyline-erythromycin (strong synergy) when used in pairs (see Figure 2).

2.4 Akaike Information Criteria and Model Selection

To statistically compare the pairwise model with the independent model, we use standard model-selection techniques [40] (see Table S1 for results). Specifically, we assume that the experimental errors are independent and Gaussian distributed with unknown variance σ^2. We confirm approximate normality of residuals in Figure S10. We then calculate for each model the Akaike Information Criteria, which is given by

$$\mathrm{AIC} = -2\log(\mathcal{L}(\hat{c}|y)) + 2n \tag{S11}$$

where $\log(\mathcal{L}(\hat{c}|y))$ is the log likelihood function, y is the data, c is maximum likelihood estimate of the free parameters of the model (in this case, σ^2), and n is the number of free parameters ($n = 1$ for both models, corresponding to the unknown error variance). The AIC is an estimate of the expectation value of the relative Kullback-Leibler (KL) divergence between the fitted model and the "true mechanism" generating the observed data. The model with the

lowest AIC value among a set of models is considered the best model in that it minimizes the KL divergence between the model and statistical mechanism underlying the data. For independent Gaussian errors, AIC reduces (up to an additive constant) to

$$\mathrm{AIC} = -N \log(\hat{\sigma}^2) + 2n, \tag{S12}$$

where N is the number of observations and $\hat{\sigma}^2$ is the maximum likelihood estimate of the variance. In practice, we use a small sample estimator of AIC that includes a bias correction term

$$\mathrm{AIC} = -2 \log(\mathcal{L}(\hat{c}|y)) + 2n + \frac{2n(n+1)}{N-n-1}. \tag{S13}$$

The differences in AIC values between the pairwise model and the Bliss independent model can be converted to an Akaiki weight in favor of the pairwise model,

$$w = \frac{\exp(-\delta/2)}{\exp(-\delta/2)+1} \tag{S14}$$

where $\delta \equiv \mathrm{AIC}_{\mathrm{pair}} - \mathrm{AIC}_{\mathrm{ind}}$. Because $\exp(-\delta/2)$ is proportional to the likelihood of the pairwise model given the data, the weight w can be interpreted as a measure of the evidence in favor of the pairwise model as the best of the two models.

2.5 Predictions of 3-Drug and 4-Drug Effects

Figures S11 - S15 show predictions for three-drug (Figures S11 - S14) and four-drug (Figure S15) combinations calculated using the maximum entropy distributions (or, equivalently, using Equation S7). Each figure includes heat maps comparing experimental growth to theoretical predictions (left hand side) as well as a direct comparison of predictions vs. experiments.

2.6 Combinatorial Experiments Testing 3-Drug Predictions

In addition to exploring the entire space of 3-drug concentrations for the drug combinations listed above, we have also performed combinatorial experiments to test the predictions of our model on a broad range of 3-drug combinations, each at a single dosage. Each combinatorial experiment involves N drugs, each at a single concentration, $D_1, D_2, ...D_N$. In each experiment, we test all $\binom{N}{3}$ possible 3-drug combinations and compare the experimental results to predictions from our pairwise model. We choose N to be 5, 6, or 7 and performed 5 combinatorial experiments yielding a total of 93 unique 3-drug combinations and 120 unique dosage combinations.

Table S3 lists all drug combinations, and the corresponding comparisons between predictions and experiment are shown in Figures S16, S17 (inset, which includes error bars). The pairwise model performs remarkably well ($R^2 = 0.95$)

and significantly outperforms the naive independence model ($R^2 = 0.29$), which demonstrates the need to account for pairwise interactions.

To estimate the frequency of pure 3-body interactions, we also include a histogram (Figure S17, main figure) of the statistical deviations from the pairwise predictions. These deviations, which cannot be statistically explained by the pairwise approximation, occur when the 95 percent confidence interval of the difference $\delta = g_{exp} - g_{pred}$, where g_{exp} is the relative growth from experiment and g_{pred} is the predicted relative growth, does not contain 0. The difference between the boundary of this confidence interval and 0 is defined to be the deviation, ΔI_3 (units are relative growth rate); this deviation may arise from pure 3-drug interactions. In 74 of the 120 drug combinations, the deviation is zero ($\Delta I_3 = 0$). In the remaining 46 combinations, the deviations (unexplained drug interactions) are very small (mean$= 0.034 \pm 0.005$), with the maximum of $\Delta I_{3,max} = 0.12$.

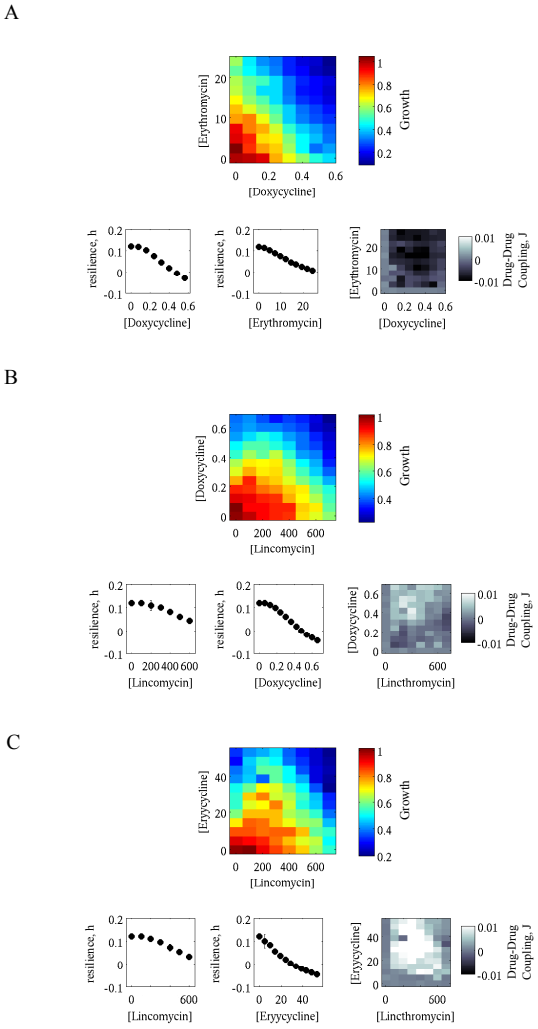

Figure S2: Experimentally determined growth rates, resilience coefficients (h), and coupling coefficients (J), of maximum entropy distribution for pairwise drug interactions. Growth rate data and maximum entropy coefficients for drug pairs (A) Doxycycline-Erythromycin (synergistic), (B) Doxycycline-Lincomycin (weakly antagonistic), and (C) Erythromycin-Lincomycin (strongly antagonistic). In each panel, top plots show heat maps of cell growth in the presence of two drugs. Cell growth is normalized by growth in the absence of drugs. Warmer colors indicate high growth rates, whereas cooler colors indicate slower growth rates. Bottom left, resilience coefficients, h, as a function of each drug in the combination. Decreasing the resilience coefficient, h, corresponds to a decrease in growth rate. Error bars: standard error of replicates (smaller than data points). Bottom right, drug-drug coupling coefficients, J, as a function of drug concentration for each drug pair. $J > 0$ corresponds to antagonism, $J < 0$ to synergy, and $J = 0$ to additivity.

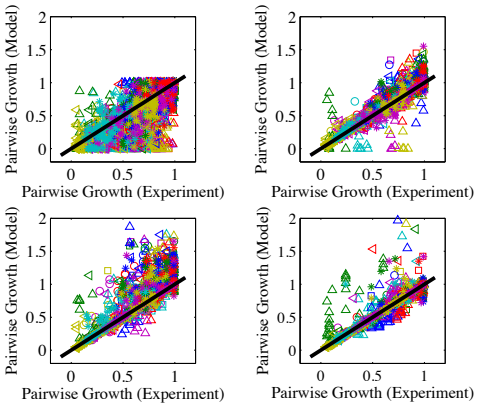

Figure S3: Fitting two-drug Data Using State Spaces with $a = 0$, $b > 0$. Upper left, $b = 1$, upper right, $b = 3$, lower left, $b = 5$, lower right, $b = 5$. Different symbols represent growth of cells in response to drug pairs drawn from different three-drug combinations (Sal-Ery-Cm, squares; Cm-Ery-Tmp, circles; Cm-Ofl-Sal, upright triangles; Cm-Ofl-Tmp, leftward triangles; Dox-Ery-Linc, stars). Black lines, line of slope 1 indicating perfect fit. Note that many data points in the lower right panel fall outside of the range of the plots.

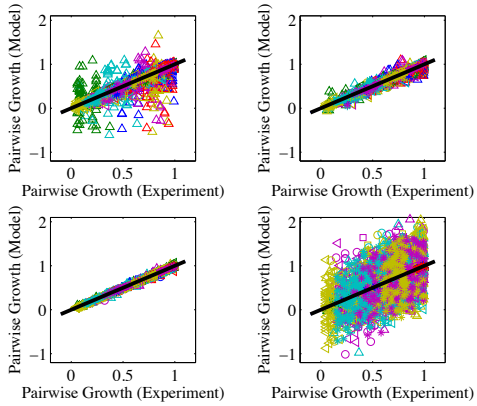

Figure S4: Fitting two-drug Data Using State Spaces with $a < 0$, $b > 0$. Upper left, $(a, b) = (-0.5, 1.5)$, upper right, $(a, b) = (-2, 3)$, lower left, $(a, b) = (-3, 4)$, lower right, $(a, b) = (-19, 20)$. Different symbols represent growth of cells in response to drug pairs drawn from different three-drug combinations (Sal-Ery-Cm, squares; Cm-Ery-Tmp, circles; Cm-Ofl-Sal, upright triangles; Cm-Ofl-Tmp, leftward triangles; Dox-Ery-Linc, stars). Black lines, line of slope 1 indicating perfect fit.

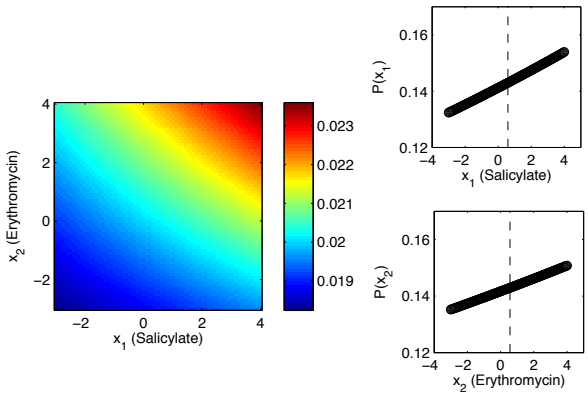

Figure S5: Example Maximum Entropy Distrubitions: Pairwise, $P_2(x_1, x_2) \equiv \int_a^b P(x_1, x_2, x_3)dx_3$ (left panel), and single variable, $P_1(x_1) \equiv \int_a^b P(x_1, x_2, x_3)dx_3dx_2$ (right panels), marginal distributions for the three-drug combination salicylate (2 mM), erythromycin (25μg/mL), and chloramphenicol (0μg/mL). Vertical dashed lines indicate averages $\langle x_i \rangle$, which correspond to single drug growth rates g_i. Drugs are arbitrarily labeled as 1 (salicylate), 2 (erythromycin), and 3 (chloramphenicol).

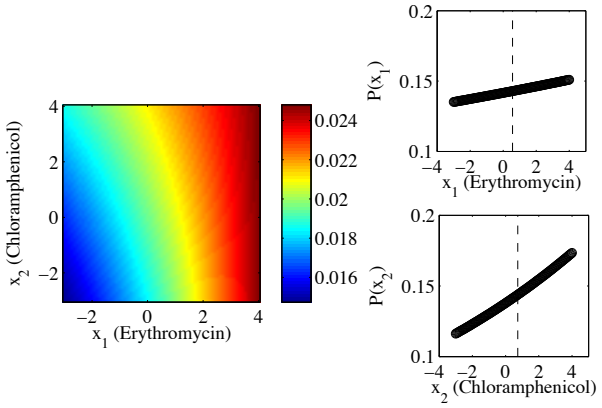

Figure S6: Example Maximum Entropy Distrubitions: Pairwise, $P_2(x_1, x_2) \equiv \int_a^b P(x_1, x_2, x_3)dx_3$ (left panel), and single variable, $P_1(x_1) \equiv \int_a^b P(x_1, x_2, x_3)dx_3dx_2$ (right panels), marginal distributions for the three-drug combination salicylate (0 mM), erythromycin (25μg/mL), and chloramphenicol (1μg/mL). Vertical dashed lines indicate averages $\langle x_i \rangle$, which correspond to single drug growth rates g_i. Drugs are arbitrarily labeled as 1 (erythromycin), 2 (chloramphenicol), and 3 (salicylate).

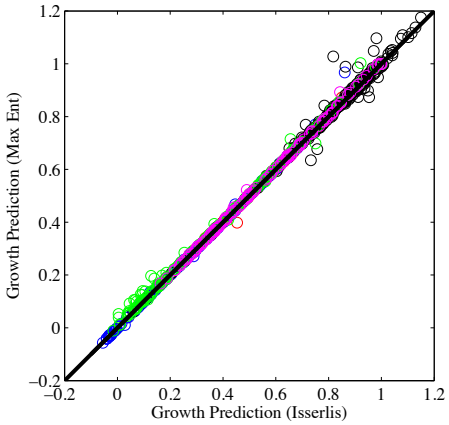

Figure S7: Comparison of Moment Relationships given by Maximum Entropy and Isserlis' Theorem: Predictions of growth in the presence of three-drug (3rd order moments) based on maximum entropy (x axis) and Isserlis' theorem (y-axis). Different colors represent different three-drug combinations.

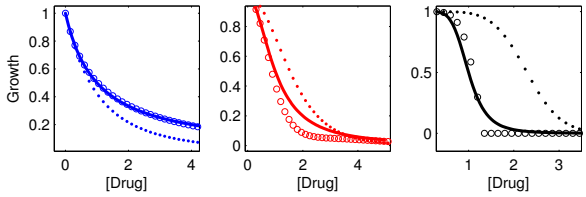

Figure S8: Drug With Itself. Predictions from Isserlis' equation (open circles) and Bliss independence (solid circles) for Hill function dose response curves (solid line) with Hill coefficients $n = 1$ (left), $n = 2$ (center), and $n = 5$ (right).

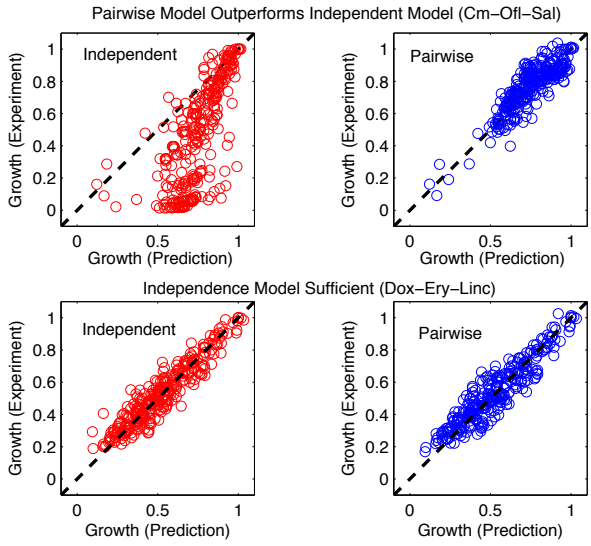

Figure S9: Comparison between independent model (left) and pairwise model (right) for two three-drug combinations: chloramphenicol-ofloxacin-salicylate (top) and doxycycline-erythromycin-lincomycin (bottom).

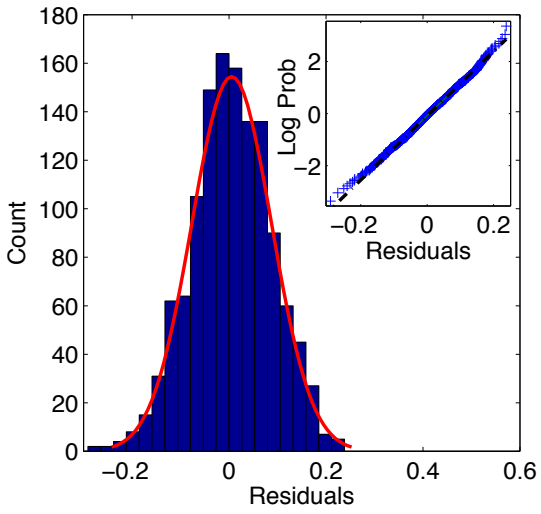

Figure S10: Verifying Normality of Residuals. Main figure, Histogram of Residuals from Pairwise Model (all drug combinations); red line, fit to normal distribution. Inset: Normal Probability Plot (straight line indicates normality).

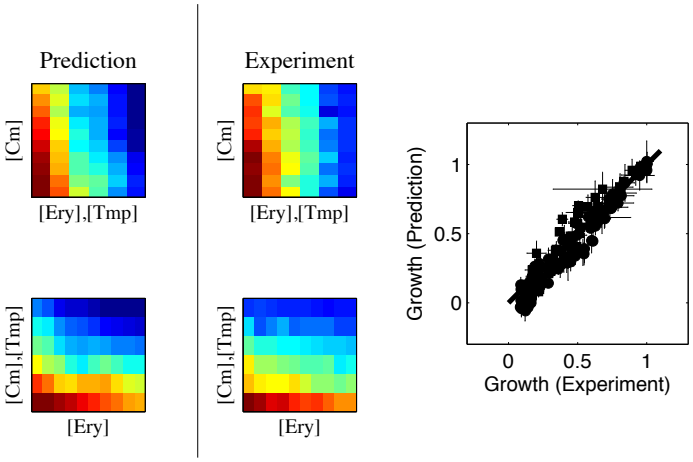

Figure S11: Comparison of Predictions with Experiments for the three-drug combination Cm-Ery-Tmp.

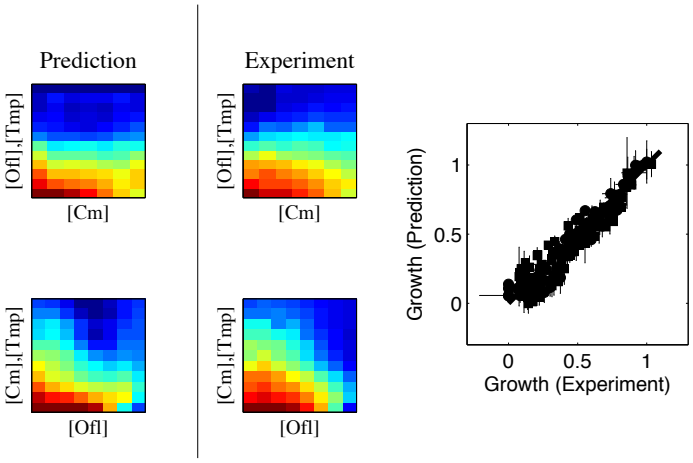

Figure S12: Comparison of Predictions with Experiments for the three-drug combination Cm-Ofl-Tmp

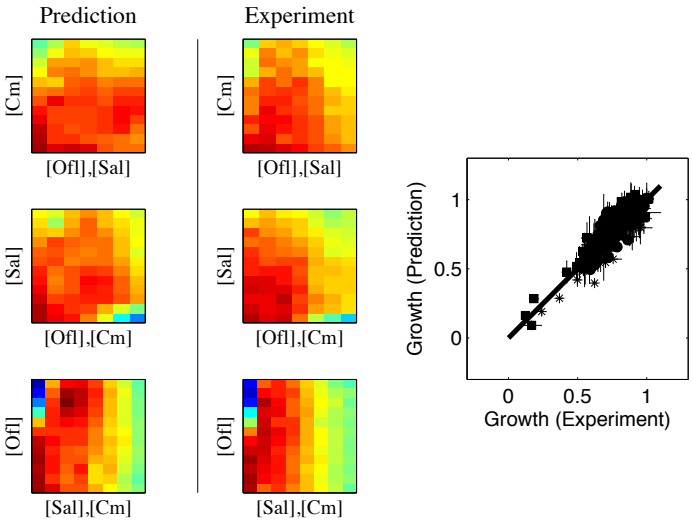

Figure S13: Comparison of Predictions with Experiments for the three-drug combination Cm-Ofl-Sal

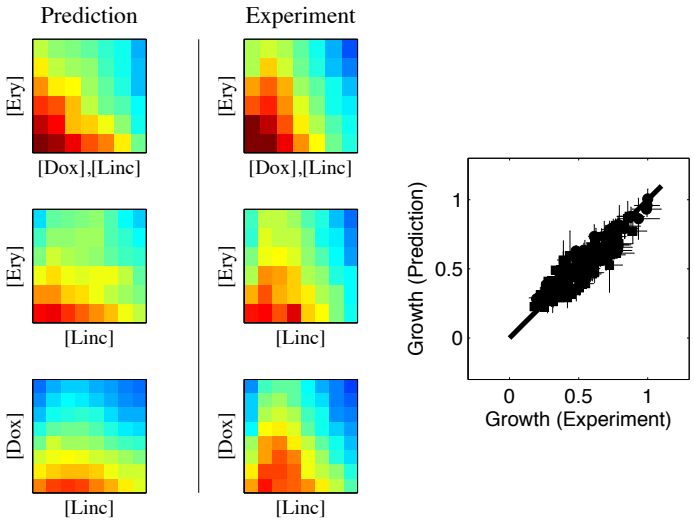

Figure S14: Comparison of Predictions with Experiments for the three-drug combination Dox-Ery-Linc

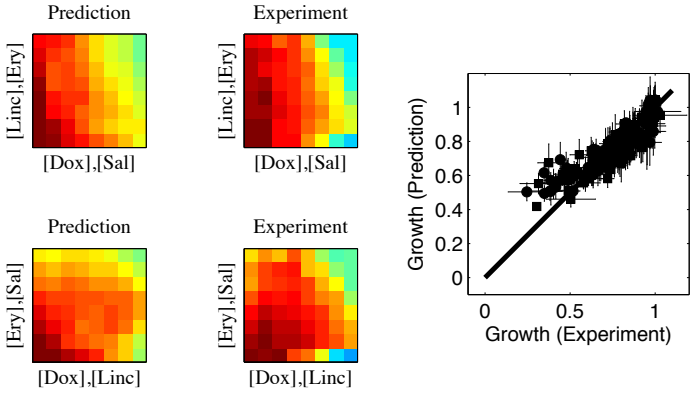

Figure S15: Comparison of Predictions with Experiments for the four-drug combination Dox-Ery-Linc-Sal

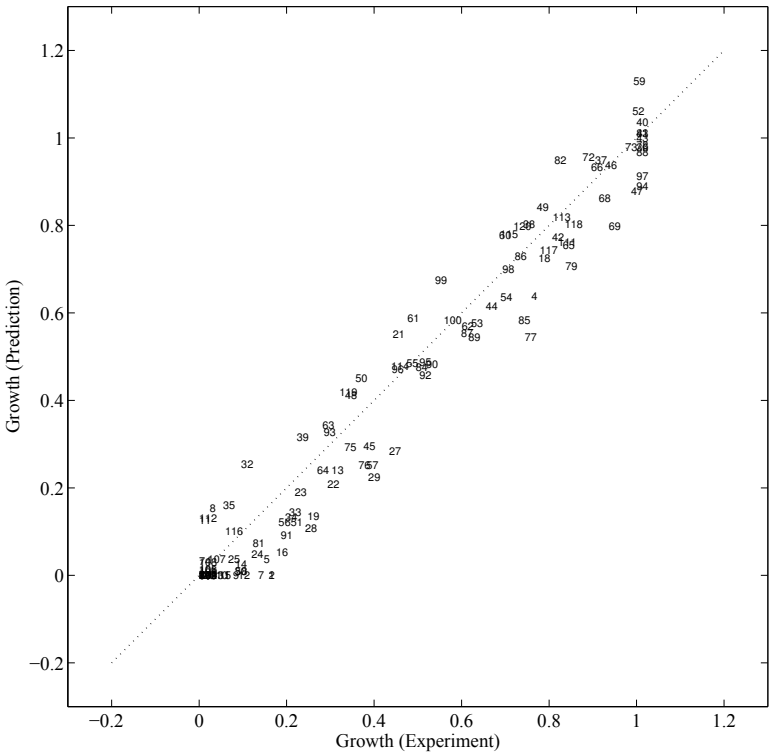

Figure S16: Comparison of Predictions with Experiments for the 3-drug Combinatorial Experiments. Each number corresponds to a 3-drug combination from the table at the end of the SI material.

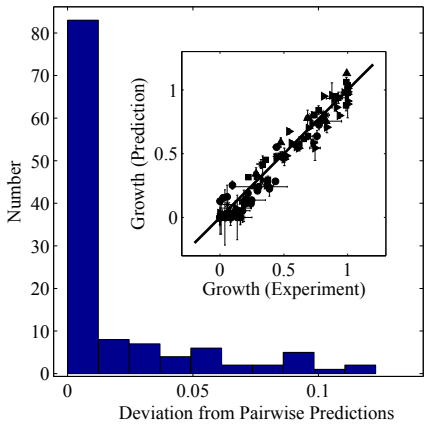

Figure S17: Histogram of Deviations from Pairwise Predictions. Deviations from the pairwise predictions occur when the 95 percent confidence interval of the difference $\delta = g_{exp} - g_{pred}$, where g_{exp} is the relative growth from experiment and g_{pred} is the predicted relative growth, does not contain 0. The difference between the boundary of this confidence interval and 0 is defined to be the deviation from pairwise predictions (units are relative growth rate). Inset: Comparison of Predictions with Experiments for the 3-drug Combinatorial Experiments. Error bars are ± standard error.

References

[33] Kapur, J N (2009), *Maximum Entropy Models in Science and Engineering*, New Age International Publishers, New Delhi.

[34] The standard Shannon measure of entropy (see, for example, [19] is a special case of this Bayesian entropy when the prior distribution is uniform.

[35] S. Kullback (1959), *Information theory and statistics*, John Wiley and Sons, NY.

[36] The traditional Ising model defines interactions between discrete spins taking values of 1 or -1. Also, it is typically assumed that the $J_{ij} = J$, independent of spin. Our model, on the other hand, resembles a continous-spin version of the disordered Ising model where both the fields h_i and the couplings J_{ij} differ for each spin.

[37] Mead, L and N Papanicolaou (1984), *Maximum Entropy in the Problem of Moments*, J. Math. Phys. 25, 2404.

[38] Isserlis, L (1916), *On Certain Probable Errors and Correlation Coefficients of Multiple Frequency Distributions with Skew Regression*, Biometrika 11: 185190.

[39] Michalowicz, J, Nichols, J, Bucholtz, J and Olson, C (2009), *A general Isserlis theorem for mixed-Gaussian random variables*, J. Stat. Phys., Volume 136 (1), 89-102.

[40] Burnham, K and Anderson, D (1998). *Model Selection and Multimodel Inference*, 2nd Edition, Springer-Verlag, New York.